Lecture 11: Charge and flux qubits

QIC880, Adrian Lupascu

(Dated: 2013/10/16)

I. THE CHARGE QUBIT

The circuit for the charge qubit is shown in Fig. 1. The traditional name for this circuit is the Cooper pair box, a name which dates from the pre-quantum computing times [1]. The circuit consists of a superconducting island coupled to an electrode through a tunnel junction and to a voltage source through a gate capacitor.

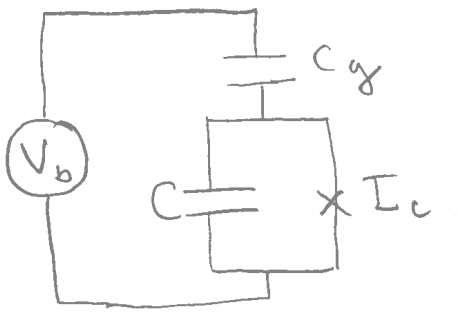

FIG. 1. Circuit for the Cooper pair box.

The subscripts for the voltages and current use in the following are "b", "J", "c", and "g" for the bias voltage source, the Josephson junction channel, the capacitance associated with the junction, and the gate capacitance respectively. The Kirchhoff's voltage and current relations are

$$V_b = V_g + V_c \tag{1}$$

$$V_c = V_J \tag{2}$$

$$I_g = I_c + I_J \tag{3}$$

which become

$$V_b = Q_g/C_g + Q_c/C \tag{4}$$

$$Q_c/C = \phi_0\dot{\gamma} \tag{5}$$

$$\dot{Q}_g = \dot{Q}_c + I_c \sin\gamma \tag{6}$$

where we introduced the phase γ over the Josepshon junction and the critical current I_c. We extract Q_g and Q from 4 and 5 and replace in 6. We find

$$C_g \dot{V}_b - \phi_0 C_g \ddot{\gamma} = \phi_0 C \ddot{\gamma} + I_C \sin\gamma. \tag{7}$$

This equation is consistent with the following Lagrangean:

$$\mathcal{L} = \frac{\phi_0^2}{2}(C + C_g)\dot{\gamma}^2 - \phi_0 C_g V_b \dot{\gamma} + \phi_0 I_c \cos\gamma. \tag{8}$$

The momentum conjugate to γ is

$$p = \phi_0 \left(C\phi_0\dot{\gamma} - C_g(V_b - \phi_0\dot{\gamma})\right). \tag{9}$$

This is, up to the constant ϕ_0, equal to the charge on two capacitors at the island side, which is the total charge on the island. This type of relation was also found in the case of a single Josephson junction and is quite generic in superconducting circuits.

We can next find the Hamiltonian, by doing the Legendre transform. We find:

$$H = \frac{1}{2}\frac{1}{\phi_0^2(C + C_g)}\left(p + \phi_0 C_g V_b\right)^2 - \phi_0 I_c \cos\gamma. \tag{10}$$

The canonical commutation relation is

$$[p, \gamma] = -i\hbar. \tag{11}$$

As

$$p = Q_{island}\frac{\hbar}{2|e|} \tag{12}$$

we have

$$p = \hbar n. \tag{13}$$

where n is the number of Cooper pair that had left the island.. We next define a quantity called "gate charge" as

$$n_g = -\frac{C_g V_b}{2|e|}. \tag{14}$$

The Hamiltonian is finally expressed as

$$H = \frac{1}{2}E_C\left(n - n_g\right)^2 - E_J\cos\gamma. \tag{15}$$

where we introduced the charging energy

$$E_c = \frac{(2e)^2}{C + C_g} \tag{16}$$

and the Josephson energy $E_J = \phi_0 I_c$.

The type of solutions that we have to consider for 15 requires further discussion. We can write the expression for the charge operator explicitly and take

$$H = \frac{1}{2} E_C \left(\frac{1}{i} \frac{d}{d\gamma} - n_g \right)^2 - E_J \cos\gamma. \tag{17}$$

Particular attention has to be paid to the properties of the solutions related to the invariance properties in terms of γ. The Hamiltonian is invariant under translations by multiples of 2π. In solid-state theory a similar problem appears when considering the Hamiltonian for electrons in a perfect crystal[2]. In that case it is found that the solutions $\psi(\gamma)$ of the time-independent Schrodinger equations have to satisfy the following property:

$$\psi(\gamma + 2\pi n) = e^{ik2\pi n} \psi(\gamma) \tag{18}$$

where k is a real number called crystal momentum or quasimomentum. In a crystal the values of the wavefunction at two equivalent points is the same, except for a phase factor. The situation is different for a Josephson junction. Two states characterized by values of γ different by multiples of 2π are in fact identical states, as recognized in [3] (see also discussion in appendix A-1 of [4]). The proper condition in this case is periodicity.

$$\psi(\gamma + 2\pi n) = \psi(\gamma). \tag{19}$$

The eigenfunctions satisfy thus the equation

$$\frac{1}{2} E_C \left(\frac{1}{i} \frac{d}{d\gamma} - n_g \right)^2 \psi(\gamma) - E_J \cos\gamma \psi(\gamma) = E\psi(\gamma) \tag{20}$$

This equation has a continuous set of eigenvalues; when we add the periodicity condition 19 the spectrum becomes discrete. The eigenfunctions are in this case the Mathieu functions (see pages 41-43 in [4]).

A different way to express the Hamiltonian 17 is

$$H = \frac{1}{2} E_C \left(n - n_g \right)^2 - \frac{E_J}{2} \sum_n \left(|n+1\rangle\langle n| + |n\rangle\langle n+1| \right). \tag{21}$$

This is the same as the Hamiltonian for a isolated Josephson junction if we take $V_b = 0$ and we take the capacitance of the junction to be $C + C_g$. It can be shown that 21 follows from 17 if we express the wavefunctions as a discrete expansion in terms of functions periodic with 2π periodicity.

A. The charge regime

This is the regime in which $E_C \gg E_C$. The first term in 21 dominates the Hamiltonian, so we consider the solutions for this term first, and then include the second one as perturbation. The eigenstates of

$$\frac{1}{2}E_C\left(n - n_g\right)^2 \tag{22}$$

(note that n is a operator and n_g is a parameter) are $|n\rangle$ with eigenvalues $E_n^0 = \frac{E_C}{2}(n-n_g)^2$. These are plotted in Fig. 2a. Crossing of levels take place at all integer and half-integer values of n_g. Energy eigenstates with charge values different by 1 cross at half-integer values of the gate charge; close to such a crossing, the Josephson energy is important, leading to an avoided crossing, as shown in Fig. 2b.

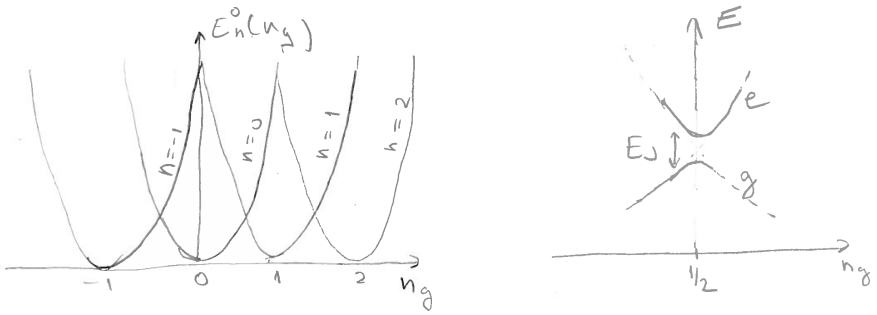

FIG. 2. a) A plot of the energy eigenstates for the charging component of the Hamiltonian, versus the gate charge. b) A plot of the energy levels for the charging component of the Hamiltonian (dashed lines) and with the Josephson energy taken into account (continuous lines), near the anticrossing at $n_g = 1/2$.

To find the energy levels we proceed as follows. We first define the gate charge $\overline{n}_g$ relative to the crossing point. In first order, the unperturbed energies around the crossing are

$$E_0^0 = \frac{E_c}{8} + \frac{E_c}{2}\overline{n}_g \tag{23}$$

and

$$E_1^0 = \frac{E_c}{8} - \frac{E_c}{2}\overline{n}_g. \tag{24}$$

We next write the Hamiltonian in the basis formed by $|0\rangle$ and $|1\rangle$:

$$H = \begin{pmatrix} \frac{E_c}{2}\overline{n}_g & -E_J/2 \\ -E_J/2 & -\frac{E_c}{2}\overline{n}_g\overline{(n)}_g \end{pmatrix}, \tag{25}$$

where we neglected a irrelevant offset. The energy eigenvalues for the ground and excited state respectively are given by

$$E_g = -\frac{1}{2}\sqrt{E_J^2 + E_c^2\overline{n}_g^2} \tag{26}$$

$$E_e = \frac{1}{2}\sqrt{E_J^2 + E_c^2\overline{n}_g^2} \tag{27}$$

The energy eigenstates are

$$|g\rangle = \cos\frac{\theta}{2}|0\rangle + \sin\frac{\theta}{2}|1\rangle, \tag{28}$$

$$|e\rangle = \sin\frac{\theta}{2}|0\rangle - \cos\frac{\theta}{2}|1\rangle \tag{29}$$

where we introduced the angle θ defined by

$$\tan\theta = -\frac{E_J}{E_c\overline{n}_g}. \tag{30}$$

Away from the symmetry point ($\overline{n}_g$ significantly different of 0) the energy eigenstates are well defined charge states. In general, the energy eigenstates are simple superpositions of charge states. This is why this type of qubit is called a *charge* qubit.

We also note that in most the designs the single Josephson junction is transformed into a DC-SQUID with small inductance. This SQUID behaves like a single Josephson junction with a critical current which is tuned by the externally applied magnetic field. This is useful as it allows one to effectively change the E_J/E_c ratio *in situ*, a useful knob for quantum control.

1. The NEC experiment - the first coherent oscillations ever observed in a solid-state device

The first coherent oscillations of a superconducting qubit, and in fact the first for a solid-state device, were observed in 1999 at NEC by Nakamura *et al.* The system used was a charge qubit in the charge regime.

The quantum control scheme was different of the usual resonant scheme used to induce transitions between states in nowadays experiments. It involved the following steps:

1. waiting time at a value of $\overline{n}_g < 0$ far from the anticrossing; the systems settles in the ground state which is given approximately by $|0\rangle$

2. fast change of $\overline{n}_g$ to 0. This change is non-adiabatic, so the state is unchanged.

3. a time is allowed at $\overline{n}_g = 0$ so that coherent oscillations take place between states $|0\rangle$ and $|1\rangle$

4. fast, non-adiabatic, change of $\overline{n}_g$ to its initial value away from the symmetry point. From here on, no oscillations between the charge states take place anymore.

5. the charge state of the qubit is measured

The non-adiabatic method for gates is not used in current experiments, as it has the following drawbacks:

1. it requires fast pulses, which spectrally contain a very wide frequency band, and thus are susceptible to dispersion. The latter is not a problem with resonant pulses.

2. the change between two operation points may be such that one particular energy eigenstate at one bias point is a linear combination of multiple (more than two) energy eigenstates at a second bias point, which leads to leakage out of the computational space

B. The tunneling regime - the transmon

The charge qubit in the $E_c \gg E_J$ has the drawback that the energy levels are strongly dependent the gate charge n_g. In mesoscopic devices charge noise is present at low frequencies. The effect of this noise is to add to the gate charge, as determined by the set voltage, a random component . Using schemes such as spin echo (this will be discussed in more detail later) the effect of this noise can be partially removed, however the remaining effects are still very damaging to coherence [5]. Fluctuations of the gate charge are not well understood and various attempts to remove them by improving device design have only been partly successful.

It has been realized relatively recently that by working in the opposite limit, $E_J \gg E_c$, the performance of the circuit as a qubit can be improved [6]. In this limit, the dependence of

the energy levels on gate becomes much weaker (this effect has already been recognized in the case of the persistent current qubit, see [7]). The drawback is the decrease in anharmonicity. Overall, one gains, because the anharmonicity decreases as a polynomial law, whereas the dependence on the gate charge decreases exponentially. Increasing the E_J/E_c ratio is done by adding a capacitance in parallel with the junction, which increases the capacitance and thus diminishes E_c.

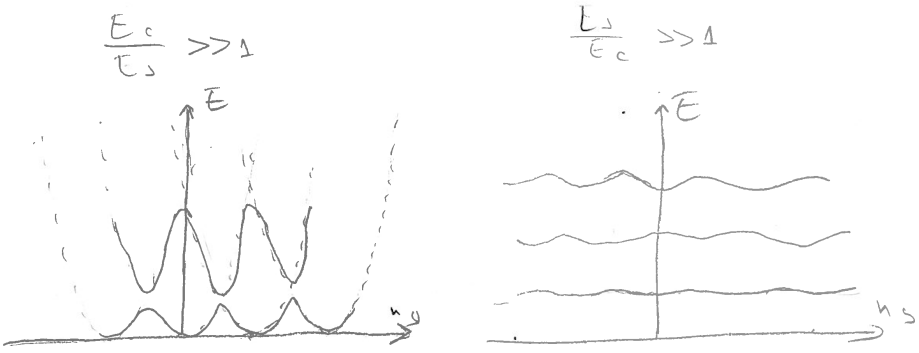

FIG. 3. A plot of the energy levels versus gate charge in two limits:large and small E_c/E_J ratio, left and right plots respectively.

II. THE FLUX QUBIT

A few different types of flux qubits exist. All these systems have in common the following features:

1. they contain one loop with at least a Josephson junction
2. the system is operated close to a half integer number of applied flux quanta, where two classical states are degenerate
3. the two lowest energy eigenstates are written as a combination of two states which have well defined value of the flux generated by the ring; the values of this flux are equal and have opposite sign

The first type of flux qubit we will consider is the 1 junction interferometer (called often the RF-SQUID despite the fact that this name suggests its operation as a magnetic field sensor).

Historically the RF-SQUID was extremely important, as it was the paradigm of *macroscopic quantum coherence* - an area of research concerned with superpositions of quantum states in a large physical system (see [8]). It was also the first system where superpositions of states were observed in an experiment [9]. The persistent current qubit (PCQ) represented another important step [7]. The PCQ removes one particular problem of the RF-SQUID: the design is such that a large loop (as needed for large inductance) is not needed, which removes the sensitivity of the system to magnetic field fluctuations.

A. The RF-SQUID

The circuit of the RF-SQUID is shown in Fig. 4. The two circuit equations are:

$$I_{ring} = I_c \sin\gamma + \phi_0 C\ddot{\gamma} \tag{31}$$

and

$$\gamma = -\frac{1}{\phi_0}\left(\Phi_x + LI_{ring}\right), \tag{32}$$

where I_{ring} is the current in the ring, γ is the phase over the junction, C is the capacitance of the junction, I_c is the critical current of the junction, and Φ_x is the externally applied magnetic flux. The Lagrangean is

$$\mathcal{L} = \frac{1}{2}\phi_0^2 C\dot{\gamma}^2 - U(\gamma) \tag{33}$$

with

$$U(\gamma) = -\phi_0 I_c \cos\gamma + \frac{\phi_0^2}{2L}\left(\gamma + 2\pi f_x\right)^2 \tag{34}$$

where $f_x = \Phi_x/\Phi_0$. The Hamiltonian is given by

$$H = \frac{1}{2}\frac{1}{\phi_0^2 C}p^2 + U(\gamma) \tag{35}$$

where p is the momentum conjugate to the phase γ.

The potential energy, shown in 5a, has many minima when the screening parameter $\beta = LI_c/\phi_0$ is large. The positions of the minima are the same as the classical solutions for the one junction interferometer, found in a previous lecture. When $f_x = 1/2$, or at equivalent half integer positions, degenerate states in the two lowest wells are strongly coupled by

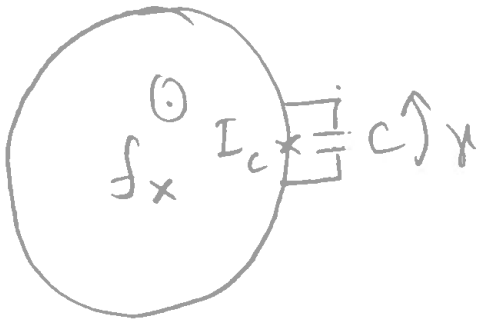

FIG. 4. The RF-SQUID circuit.

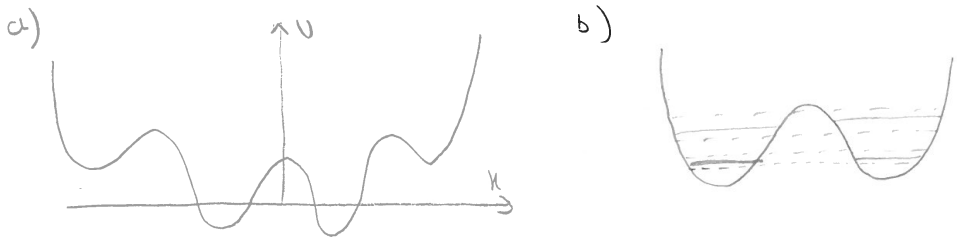

FIG. 5. a) The potential energy of the RF-SQUID. b) Schematic representation of the energy states at $f_x = 1/2$. The continuous lines are quasi-energy eigenstes localized in each well; the dashed lines are the proper states with tunneling taken into account.

tunneling across the potential. The basis states, which are the minimum energy harmonic-oscillator like states, have a magnetic flux expectation value which is $\pm\Phi_0/2$.

The structure of the Hamiltonian 35 is such that there is no periodicity in changes of γ by multiples of 2π. For this reason, the wavefunctions are no longer required to be periodic in the phase γ.

B. The persistent current qubit

The PCQ circuit is shown in Fig. 6a. The circuit consists of a loop with very small self inductance and interrupted by three Josephson junctions, two of which are equal in parameters (Josephson energy E_J and charging energy E_c) and the third having a junction barrier area α times the size of the first two junction (so it has Josephson energy αE_J and charging energy $\alpha^{-1}E_c$). Using reasoning very similar to the analogous derivation for the

RF-SQUID, the Hamiltonian is given by

$$H = \frac{\hbar^2}{2} E_c (p_1^2 + p_2^2 + \alpha^{-1} p_3^2) + U(\gamma_1, \gamma_2, \gamma_3), \tag{36}$$

with p_1, p_2, and p_3 the momenta conjugate to the phases γ_1, γ_2, and γ_3 over the three junctions, and the potential energy

$$U(\gamma_1, \gamma_2, \gamma_3) = -E_J(\cos\gamma_1 + \cos\gamma_2 + \alpha\cos\gamma_3) + \frac{\phi_0^2}{2L}\left(\gamma_1 + \gamma_2 + \gamma_3 + 2\pi f_x\right)^2 \tag{37}$$

with f_x the external frustration in the ring.

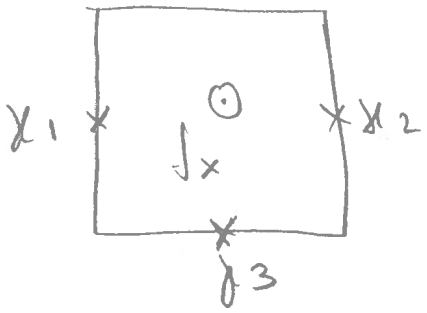

FIG. 6. a)The PCQ circuit.

The following simplification is possible for the Hamiltonian 36. Since the inductance L is extremely small, low energy states are obtained when the quadratic part in the potential energy 37 is at its minimum; this is achieved by taking $\gamma_1+\gamma_2+\gamma_3+2\pi f_x = 0$. This constraint can be introduced before deriving the Lagrangian, and only two degrees of freedom, γ_1 and γ_2, are retained. With this, the Hamiltonian becomes

$$H = \frac{\hbar^2}{2} E_c \boldsymbol{p} \tilde{C}^{-1} \boldsymbol{p}^T + U(\gamma_1, \gamma_2), \tag{38}$$

with $\boldsymbol{p} = (p_1, p_2)$ the set of momenta conjugate to the two phases and the matrix

$$\tilde{C} = \begin{pmatrix} 1+\alpha & \alpha \\ \alpha & 1+\alpha \end{pmatrix}. \tag{39}$$

The potential energy

$$U(\gamma_1, \gamma_2) = -E_J\left(\cos\gamma_1 + \cos\gamma_2 + \alpha\cos\left(2\pi f_x + \gamma_1 + \gamma_2\right)\right). \tag{40}$$

This energy is invariant under translations by 2π in either direction. A plot of the potential energy is shown in Fig. 7. Around $f_x = 0.5$ two potential wells exist in each unit cell. Each well has a eigenenergy state, with the same energy for $f_x = 0.5$ (see Fig. 7a). These two states have well defined values of the phase, and therefore well defined values of the generated flux. The two states have clockwise/anticlockwise currents. When $f_x > 0.5$, the anticlockise current state has lower energy (see Fig. 7b); when $f_x < 0.5$ the clockwise current state has lower energy. As for the case of the RF SQUID, tunneling between the two well leads to avoided crossing.

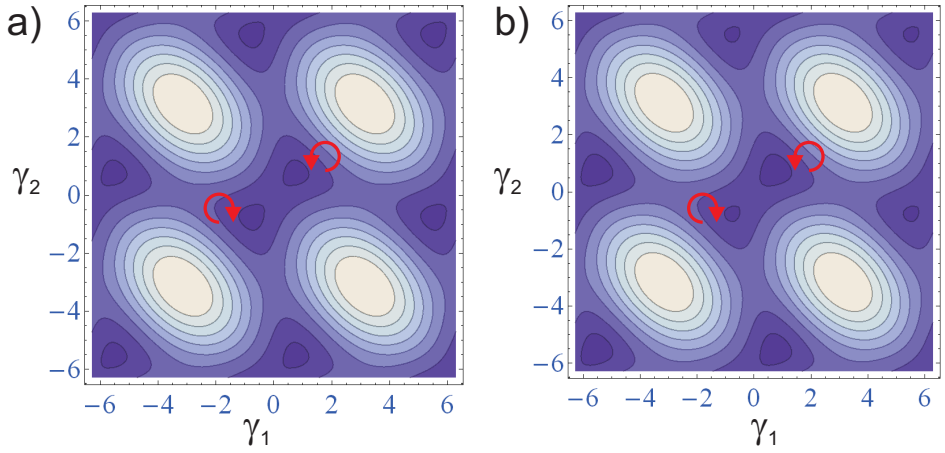

FIG. 7. A plot of the potential energy for the PCQ with $f_x = 0.5$ (a) and $f_x = 0.509$ (b). The lines are equipotential contours. The arrows indicate the direction of the loop current corresponding to each minima.

A numerical solution for the energy eigenvalues is given in 8. The PCQ is found to have very large anharmonicity, which is an advantage for quantum control. The space formed by the lowest two levels is well described by the Hamiltonian

$$H_{\text{PCQ, 2-state}} = -\frac{\Delta}{2}\sigma_x - \frac{\epsilon}{2}\sigma_z \tag{41}$$

with Δ the minimum energy level splitting and

$$\epsilon = 2I_p(\Phi - \Phi_0/2) \tag{42}$$

with I_p the persistent current of the qubit (this is the value of the current corresponding to each classical state).

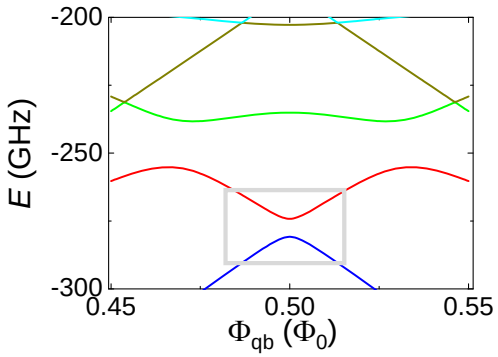

FIG. 8. A plot of the first few energy levels for a PCQ with typical parameters.

[1] V. Bouchiat, D. Vion, P. Joyez, D. Esteve, and M. Devoret, Physica Scripta **1998**, 165 (1998).

[2] N. W. Ashcroft and N. D. Mermin, *Solid State Physics* (Harcourt College Publishing, 1976).

[3] K. Likharev and A. Zorin, Journal of low temperature physics **59**, 347 (1985).

[4] A. Cottet, *Implementation of a quantum bit in a superconducting circuit*, Ph.D. thesis, CEA Saclay (2003).

[5] Y. Nakamura, Y. Pashkin, T. Yamamoto, and J. Tsai, Phys. Rev. Lett. **88**, 47901 (2002).

[6] J. Koch, T. M. Yu, J. Gambetta, A. A. Houck, D. I. Schuster, J. Majer, A. Blais, M. H. Devoret, S. M. Girvin, and R. J. Schoelkopf, Phys. Rev. A **76**, 042319 (2007).

[7] J. E. Mooij, T. P. Orlando, L. Levitov, L. Tian, C. H. van der Wal, , and S. Lloyd, Science **285**, 1036 (1999).

[8] A. J. Leggett and A. Garg, Phys. Rev. Lett. **54**, 857 (1985).

[9] J. Friedman, V. Patel, W. Chen, S. Tolpygo, and J. Lukens, Nature **406**, 43 (2000).